Inverse Reconstruction Method for Segmented Multishot Diffusion-Weighted MRI With Multiple Coils

Martin Uecker,* Alexander Karaus, and Jens Frahm

Each *k*-space segment in multishot diffusion-weighted MRI is affected by a different spatially varying phase which is caused by unavoidable motions and amplified by the diffusion-encoding gradients. A proper image reconstruction therefore requires phase maps for each segment. Such maps are commonly derived from two-dimensional navigators at relatively low resolution but do not offer robust solutions. For example, phase variations in diffusion-weighted MRI of the brain are often characterized by high spatial frequencies. To overcome this problem, an inverse reconstruction method for segmented multishot diffusion-weighted MRI is described that takes advantage of the full *k*-space data acquired from multiple receiver coils. First, the individual coil sensitivities are determined from the non–diffusion-weighted acquisitions by regularized nonlinear inversion. These coil sensitivities are then used to estimate accurate motion-associated phase maps for each segment by iterative linear inversion. Finally, the coil sensitivities and phase maps serve to reconstruct artifact-free images of the object by iterative linear inversion, taking advantage of the data of all segments. The efficiency of the new method is demonstrated for segmented diffusion-weighted stimulated echo acquisition mode MRI of the human brain. Magn Reson Med 62:1342–1348, 2009.

Key words: multishot diffusion-weighted imaging; inverse problems; iterative reconstruction; parallel imaging; nonlinear inversion; stimulated echo acquisition mode

In MRI, segmented *k*-space acquisitions are often attractive because they reduce the length of an acquired echo train. For example, in echo-planar-imaging a shorter train of gradient echoes translates into reduced susceptibility artifacts, while in rapid stimulated echo acquisition mode (STEAM) MRI, fewer stimulated echoes yield higher flip angles and an improved signal-to-noise ratio (SNR), as recently demonstrated for black-blood cardiac MRI (1). Unfortunately, however, segmented multishot acquisitions are not easily applicable to diffusion-weighted (DW) MRI. This is because of the occurrence of spatially varying (nonlinear) phase variations, which are caused by unavoidable nonrigid brain pulsations and patient movements during the action of the self-compensating diffusion-encoding gradients. This phase information differs for each segment and therefore prohibits a direct image reconstruction by a simple combination of all *k*-space data.

Current attempts to reconstruct motion-affected segmented *k*-space data make use of low-resolution phase maps that are either obtained by a two-dimensional navigator acquisition (2–4) or extracted from the fully sampled center of a self-calibrating *k*-space trajectory (5–7). As a common feature, these techniques rely on the assumption that the motion-associated phase varies only smoothly, so that it can be accurately described by low spatial frequencies. In DW MRI of the human brain, this condition is not generally fulfilled. A robust and artifact-free image reconstruction from segmented *k*-space acquisitions therefore requires high-resolution phase maps. These experimental approaches, however, face shortcomings: For DW echo-planar-imaging, a large two-dimensional navigator may be compromised by susceptibility problems that limit the accuracy of the resulting phase maps, while for DW STEAM MRI, the need for multiple navigator acquisitions would eliminate the SNR advantage of a shortened echo train.

In this work, an alternative solution is presented that is based on an iterative inverse image reconstruction technique that exploits the information from the entire *k*-space, as well as from multiple receiver coils. The new method allows for the reconstruction of DW images from segmented *k*-space acquisitions without motion-induced artifacts and without the need for additional navigator acquisitions. It provides a more general and robust solution than a recent proposal by Skare and colleagues (8), which relies on a standard noniterative sensitivity encoding (SENSE) or generalized autocalibrating partially parallel acquisition (GRAPPA) reconstruction and a homogeneously sampled echo-planar-imaging trajectory.

THEORY

Segmented DW MRI Using Multiple Coils

The MRI signal obtained from N receiver coils is given by

$$s_j(t) = \int \mathrm{d}\vec{x} e^{i\vec{k}(t)\vec{x}} \rho(\vec{x}) c_j(\vec{x}) \quad j = 1, \cdots, N \qquad [1]$$

Here, ρ denotes the spin density, c_j the coil sensitivities, and $\vec{k}(t)$ the *k*-space trajectory. In DW MRI, as in many other imaging scenarios, phase effects have to be taken into account by including nontrivial phase maps

$$s_{lj}(t) = \int \mathrm{d}\vec{x} e^{i\vec{k}_l(t)\vec{x}} \rho(\vec{x}) e^{ip_l(\vec{x})} c_j(\vec{x}) \quad \begin{matrix} j=1,\ldots,N \\ l=1,\ldots,M \end{matrix} \qquad [2]$$

The index describes the segment l of a multishot acquisition with M segments. Because in DW MRI the phase information is not consistent between different segments, the situation requires individual phase maps $e^{ip_l(\vec{x})}$ for each segment l. In most current approaches, phase maps and coil sensitivity maps are obtained with the use of a two-dimensional navigator acquisition or from additional autocalibration lines in the *k*-space center. Given those maps, the resulting reconstruction problem is linear and

Biomedizinische NMR Forschungs GmbH am Max-Planck-Institut für biophysikalische Chemie, Göttingen, Germany

*Correspondence to: M. Uecker, Biomedizinische NMR Forschungs GmbH, 37070 Göttingen, Germany. E-mail: muecker@gwdg.de

Received 23 December 2008; revised 30 April 2009; accepted 1 June 2009.

DOI 10.1002/mrm.22126

Published online 24 September 2009 in Wiley InterScience (www.interscience.wiley.com).

can be solved with iterative methods such as conjugate gradient–based versions of SENSE.

Recently, new algorithms for autocalibrated parallel imaging were presented, which combine the estimation of the coil sensitivities c_j and the calculation of the image ρ into a nonlinear reconstruction problem (9,10). The advantage of these nonlinear inversion techniques, namely, a better estimation of both the image and coil sensitivities, is that they allow for higher reduction factors and fewer autocalibration lines than linear inversion techniques. In a similar way, nonlinear inversion might be helpful to improve the phase maps in multishot DW MRI as the approach would include the entire available k-space data, instead of relying on a small number of navigator echoes. In fact, after only minor adjustments of the nonlinear inversion algorithm presented earlier (10), its application to DW MRI emerged as a generic alternative to conventional reconstruction methods. Despite some advances, however, the algorithm did not yield completely satisfactory results for data sets with pronounced high-frequency phase variations. For this reason, this work presents the development of a new multistep algorithm, which allows one to robustly reconstruct even severely motion-disturbed data. Because the first step of the procedure relies on regularized nonlinear inversion for autocalibrated parallel imaging (10), the respective algorithm will be briefly summarized in the next section.

Regularized Nonlinear Inversion

In regularized nonlinear inversion, the signal equation is treated as a nonlinear operator equation that maps the unknown spin density ρ and coil sensitivities c_j to the data acquired from all coils and segments

$$F : x := (\rho, c_1, \cdots, c_j) \mapsto (s_1, \cdots, s_j) \qquad [3]$$

The operator is given by

$$F : x \mapsto \begin{pmatrix} P\mathcal{F}\{c_1 \cdot \rho\} \\ \vdots \\ P\mathcal{F}\{c_N \cdot \rho\} \end{pmatrix} \quad \text{with} \quad x = \begin{pmatrix} \rho \\ c_1 \\ \vdots \\ c_N \end{pmatrix} \qquad [4]$$

where $\mathcal{F}$ is the (multidimensional) Fourier transform and P is the orthogonal projection onto the trajectory. This nonlinear equation is then solved with the iteratively regularized gauss newton method (11). Starting from an initial guess and in order to achieve an improved estimation x_{k+1}, each iteration solves the following optimization problem that corresponds to a regularized linearization of the operator equation around the current estimate x_k:

$$x_{k+1} - x_k = \operatorname{argmin}_{\delta x}\{\|DF(x_k)\delta x + F(x) - y\|_2^2 + \alpha_k \|W(x_k + \delta x - x_0)\|_2^2\}. \qquad [5]$$

Here, DF denotes the derivative of the operator F, which can be calculated by using the linearity of the Fourier transform and the product rule of derivatives

$$DF(x)\begin{pmatrix} d\rho \\ dc_1 \\ \vdots \\ dc_N \end{pmatrix} = \begin{pmatrix} P\mathcal{F}\{\rho \cdot dc_1 + d\rho \cdot c_1\} \\ \vdots \\ P\mathcal{F}\{\rho \cdot dc_N + d\rho \cdot c_N\} \end{pmatrix} \qquad [6]$$

The weighting matrix W penalizes high frequencies in the coil sensitivity part of x with the use of $(1 + a \cdot \|k\|^2)^l$ and properly chosen constants. For the object part, W contains the identity matrix, which leads to a conventional L_2-regularization for the image. The degree of regularization is reduced in each iteration according to $\alpha_k = \alpha_0(\frac{2}{3})^k$. The total number of iterations determines the final regularization, which controls the tradeoff between noise and artifact.

The algorithm is applicable to arbitrary sampling patterns or k-space trajectories as long as the k-space center is fully sampled. It makes optimal use of all receiver coils and utilizes all acquired k-space data, including reference lines for image reconstruction. A fundamental property of the weighting matrix W, which renders the algorithm capable of solving the bilinear problem for the coil sensitivity maps c_j and the image at the same time, is the assumption that the coil sensitivities are much smoother than the image.

Adaptation to Segmented MultiShot DW MRI

By combining the coil sensitivities c_j and the motion-associated phase maps e^{ip_l} into $N \times M$ generalized maps $cp_{lj}(\vec{x}) = e^{ip_l(\vec{x})} \cdot c_j(\vec{x})$, the mathematical problem becomes identical to that of autocalibrated parallel imaging. In fact, when including a low number of reference lines in each segment of a multishot acquisition, the regularized nonlinear inversion algorithm may be directly applied for image reconstruction. The implicit combination of the coil sensitivity maps and motion-associated phase maps, however, is physically unmotivated as the occurrence of high spatial frequencies in the phase maps violates the assumption of spatial smoothness for the coil profiles. It nevertheless turns out that a proper choice of the weighting matrix W offers better image quality than obtainable by a simple navigator-based approach.

An improved solution may be achieved with the use of a two-step procedure. First, the non-DW images are reconstructed by parallel imaging using nonlinear inversion. This step also yields respective coil sensitivity maps, which in a subsequent step are exploited to calculate individual images for each segment by iterative linear inversion. These images have the same motion robustness as any other single-shot acquisition, so that a final image may be calculated by averaging the magnitude images from all segments. This two-step method mimics the ideas developed for DW echo-planar-imaging by Skare et al. (8) but differs in the use of the nonlinear inversion algorithm to obtain optimum coil sensitivities in the first step. In general, however, the ill-conditioned parallel image reconstructions for individual segments lead to a high noise amplification, which affects the SNR of the final combined image.

For this reason, the above two-step method was complemented by another parallel image reconstruction process based on iterative linear inversion. This third step replaces the simple averaging of images from all segments by a true

reconstruction of the final image and therefore takes advantage of all data from all segments and coils. The required phase maps for each segment are obtained from the images calculated in the second step and possess the same resolution as the final image. The algorithm retains the motion robustness of the two-step method while avoiding its inherent noise amplification. Thus, the proposed three-step method comprises three consecutive calculations:

(1) In a first step, a non-DW image, that is, an image without diffusion encoding but otherwise identical acquisition parameters, is reconstructed from the data of all segments by regularized nonlinear inversion, as described above. In this step, all phase issues are ignored. This is possible because the relevant brain motions do not give rise to pronounced phase variations in the absence of diffusion-encoding gradients. The algorithm simultaneously recovers a high-quality image and sensitivity profile for each receiver coil.

(2) In a second step, complex-valued DW images are reconstructed separately for each segment (and all diffusion directions) by linear inversion, that is, with the use of an iterative conjugate-gradient version of the SENSE algorithm. This calculation takes advantage of the coil sensitivities c_j determined in the first step.

(3) In a third step, real-valued DW images are reconstructed from the data of all segments, again by iterative SENSE. This resonstruction uses the coil sensitivities c_j from the first step and the phase maps e^{ip_l} that are available from the images of each segment in the second step. This final step is similar to navigator-based reconstructions but differs in its use of motion-associated phase maps with much higher spatial resolution.

Taken together, the first step serves to calculate the coil sensitivity maps while ignoring phase problems, the second step estimates high-resolution phase maps that represent motion-associated phase variations (for each segment), and the third step calculates real-valued images (combining the data of all segments) by using the previously determined coil sensitivities and phase maps.

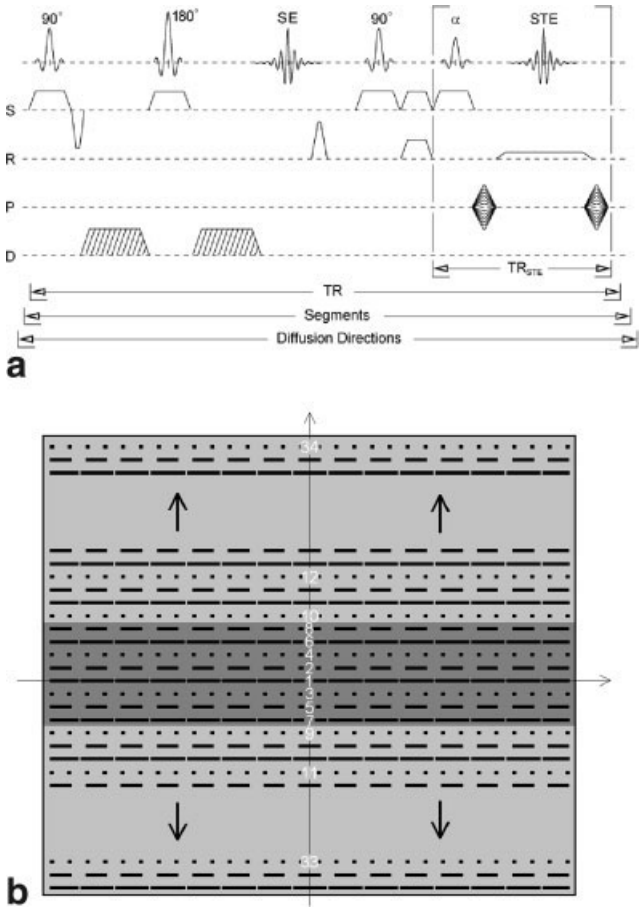

FIG. 1. **a:** Schematic diagram of a segmented multi-shot STEAM diffusion tensor imaging sequence comprising an initial spin-echo (SE) diffusion module and a high-speed STEAM MRI sequence. The sequence generates differently phase-encoded stimulated echoes (STE) by repeating the final readout interval with variable low-flip angle RF pulses (α, repetition time TR_{STE}). The acquisition of multislice diffusion-weighted images is repeated for multiple segments and different diffusion-encoding gradient directions (repetition time TR). **b:** Coverage of (segmented) k-space for Cartesian encoding with centric reordering. The example refers to the acquisition of 84 Fourier lines with the use of three segments and eight reference lines. For details see text.

MATERIALS AND METHODS

Experiments were performed at 3Tesla(T) (TIM Trio; Siemens Healthcare, Erlangen, Germany) using either an eight-channel or 32-channel phased-array head coil. Apart from preliminary studies of water phantoms, applications involved diffusion tensor imaging of the brain of young healthy adults. Written informed consent was obtained from all subjects prior to the examination.

Segmented DW MRI was based on a rapid STEAM MRI sequence (12,13) without cardiac gating. As shown in Fig. 1a, the first 90° pulse of the STEAM sequence is replaced by a spin-echo diffusion module 90° − DW − 180° − DW − spin-echo, while the final acquisition part is repeated in order to generate n stimulated echoes (STE) — corresponding to n Fourier lines — for each segment. This readout interval employs radiofrequency pulses with variable flip angles to ensure similar signal strengths for each stimulated echo. The flip angles may be iteratively calculated according to

$$\alpha_{i-1} = \arctan(\sin\alpha_i)\cdot e^{-TR/T_1} \quad [7]$$

with $\alpha_n = 90°$ and T_1 the spin-lattice relaxation time. For studies of the human brain, T_1 was chosen to be 800 ms for white matter at 3 T.

Diffusion tensor imaging was performed at 2-mm isotropic spatial resolution using one non-DW image and 24 DW images with b values of 1000 s mm^{-2} along different directions. A total of 51 transverse-to-coronal 2-mm-thick sections (orientation along the anterior to posterior commissure) covered the brain with a rectangular 168 × 192 mm^2 field of view and a matrix of 84 × 96 complex data points (corresponding to a full Fourier acquisition). For display purposes, individual DW images were mildly processed by adaptive filtering, taking into account the local intensity distribution and continuation of structures (software supplied by the manufacturer).

The coverage of k-space by segmented acquisitions with central reference lines is illustrated in Fig. 1b. The example refers to the case of three segments and eight reference

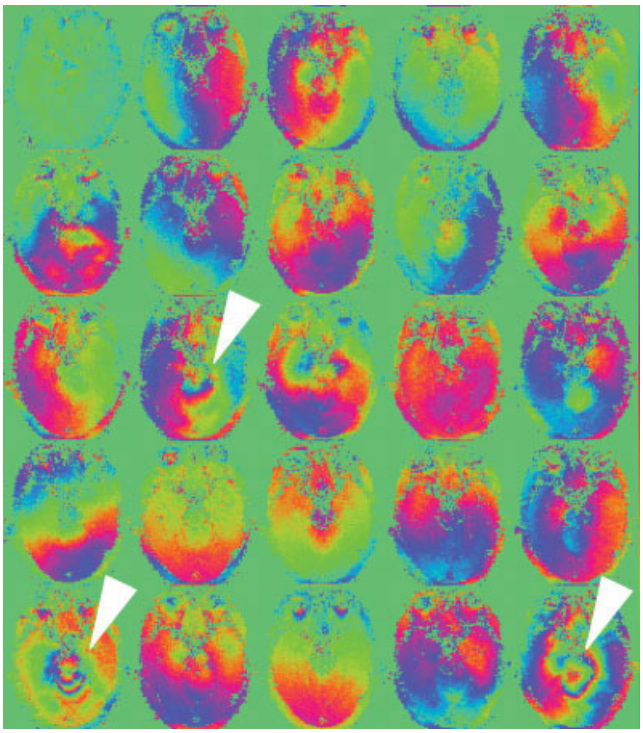

FIG. 2. Motion-associated phase maps from a four-segment DW MRI data set of the human brain (single section). The images were obtained during application of the second step of the proposed three-step method. They represent a non-DW image (upper left corner) and all DW images ($b = 1000\,\mathrm{s\,mm^{-2}}$, 24 directions) for one selected segment. The color encodes phase values between 0 and 2π. Some images are affected by marked phase changes with high spatial frequencies (arrows).

lines. For the abovementioned image matrix, three segments reduce the number of *k*-space lines (stimulated echoes) per segment from 84 to 33 or 34. While a simple division would lead to 28 lines that homogeneously cover the entire *k*-space, the use of eight reference lines adds five or six more lines, not counting those lines that are already included in the original 28 lines.

For the sequence with three segments and eight reference lines, the repetition time per segment was 15.3 s for 51 sections. The corresponding measuring time was 19 min for a diffusion tensor imaging data set with 24 diffusion directions. Studies with four segments and 16 reference lines yielded 33 lines per segment, a repetition time of 15.0 s, and a measuring time of 25 min. The total reconstruction time on a computer with two quad-core central processing units was 7 min for the three-segment data set with eight channels and 30 min for the four-segment data set with 32 channels.

The non-DW images were obtained with nonlinear inversion using weights for the coil sensitivities that were calculated according to $(1 + 225 \cdot \|\vec{k}\|^2)^{16}$. The initial regularization parameter was set to $\alpha_0 = 1$ and reduced in each step of the four-step iteration process. The linear inversion algorithm for the estimation of the DW images for individual segments was regularized with $\alpha = 0.1$. The final reconstruction of the combined DW image from all segments employed a regularization with $\alpha = 0.01$. This iteration process was stopped when the residual became smaller than 10^{-4}.

RESULTS

Figure 2 shows motion-associated phase maps for a selected section and one segment of a four-segment DW MRI data set of the human brain. These maps were estimated according to the second step of the proposed reconstruction algorithm, taking into account the coil sensitivity maps obtained in the first step. The phase maps refer to the non-DW image (upper left corner) and 24 DW images. The color code facilitates the recognition of major phase changes. The absence of any visible phase variations in the non-DW image confirms the assumption of a constant phase in the first step, that is, for the determination of the coil sensitivities from the non-DW acquisitions by regularized nonlinear inversion. While most DW images lead to maps with only moderate phase variations, some images are affected by phase changes with high spatial

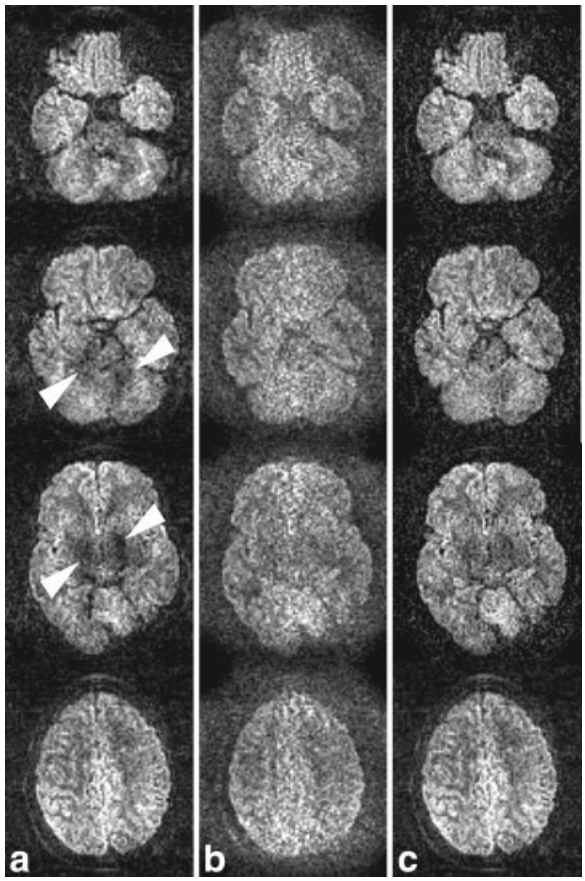

FIG. 3. DW images ($b = 1000\,\mathrm{s\,mm^{-2}}$, four sections) reconstructed from a three-segment DW MRI data set of the human brain with the use of (**a**) a direct application of the nonlinear inversion algorithm, (**b**) a two-step approach averaging the magnitude images reconstructed for individual segments, and (**c**) the proposed three-step method. The motion-induced signal void obtained for the first approach (arrows) is avoided by the more complex strategies, while the three-step method further reduces the sensitivity of the two-step approach to noise.

frequencies (arrows). In particular, this applies to the vicinity of the brain stem where brain pulsations are most pronounced.

Figure 3 compares the performance of three different reconstruction techniques for four selected sections of a three-segment acquisition. The results shown in Fig. 3a represent a direct application of the nonlinear inversion algorithm. It yields the final DW image in only one reconstruction step but merges the information from the coil sensitivities and phase variations into a single map. In this case, the images still suffer from residual motion artifacts (some signal void, arrows). Such problems are avoided by the two- and three-step methods shown in Fig. 3b and c, respectively. However, because the two-step method averages the noise-affected magnitude images from the individual segments, the final DW images (Fig. 3b) exhibit a lower SNR than the images obtained by the proposed three-step method (Fig. 3c) in spite of an identical regularization.

The general performance of the new method is demonstrated in Figs. 4 and 5 for a three- and four-segment acquisition, respectively. Figure 4 summarizes 24 of 51 DW images of a multislice data set for a single diffusion direction (Fig. 4a), as well as all 24 DW images of a single section (Fig. 4b). Finally, using the proposed algorithm, Fig. 5 shows non-DW images, DW images for one diffusion direction, isotropically DW images, and maps of the fractional anisotropy for four selected sections.

DISCUSSION

It is common knowledge that segmented multishot DW MRI is affected by motion-associated phase differences that preclude the reconstruction of artifact-free images by a straightforward combination of respective *k*-space segments. Here it is demonstrated that the typical phase variations in DW MRI of the human brain that are due to cardiac-induced brain pulsations and residual subject movements cannot be represented by low-resolution *k*-space data, as usually obtained from (external) navigator acquisitions or (internal) autocalibration or reference lines. Instead, a substantial fraction of DW images presents with phase variations that have to be characterized at full spatial resolution using the entire available *k*-space data.

In a first attempt, the direct application of a regularized nonlinear inversion algorithm turned out to be suboptimal as it forces smooth (low-resolution) coil sensitivities and irregular (high-resolution) motion-associated phase maps into a single "reference" map that complements the image of the true object. An improvement was achieved by a two-step procedure that first reconstructs the non-DW images by nonlinear inversion and then exploits the respective coil sensitivities to obtain DW images for all segments with the use of an iterative SENSE-like algorithm. However, when simply averaging the magnitude images of the individual segments to calculate the desired DW image (8), then the

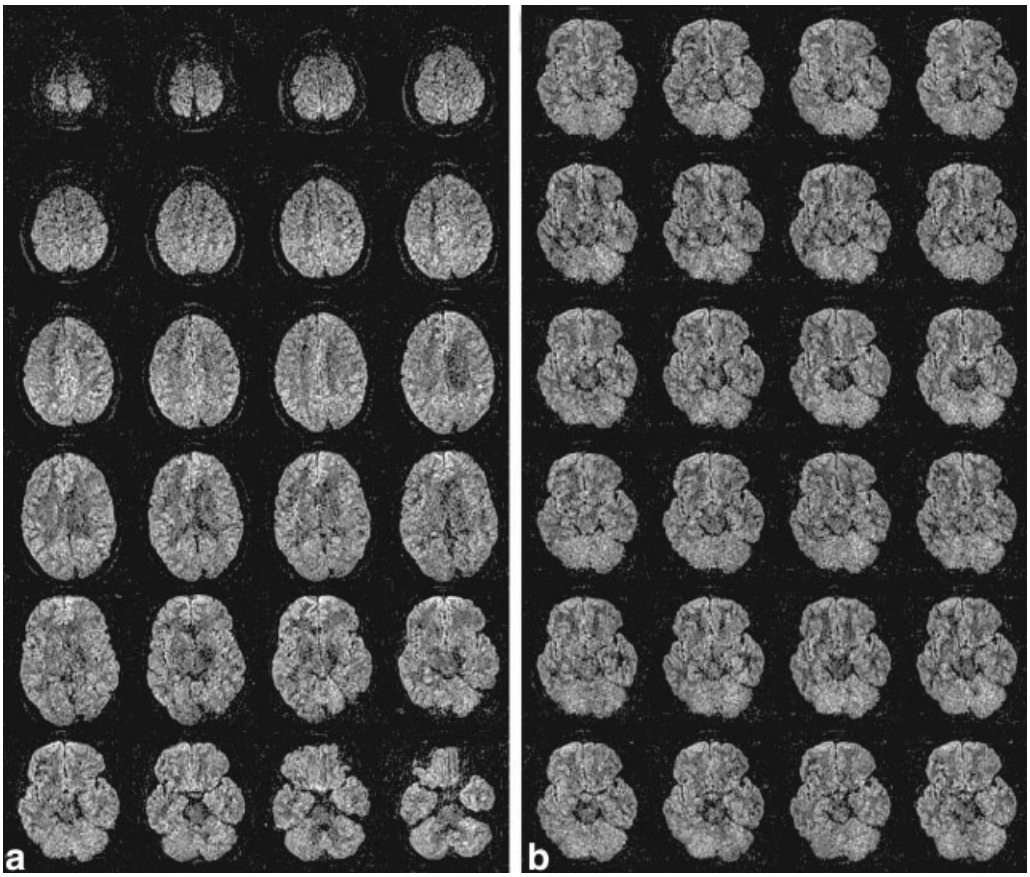

FIG. 4. **a:** Selected 24 of 51 multislice DW images for a single diffusion direction and (**b**) all 24 DW images of a single section (b = 1000 s mm^{-2}) reconstructed from a three-segment DW MRI data set of the human brain with the proposed three-step method.

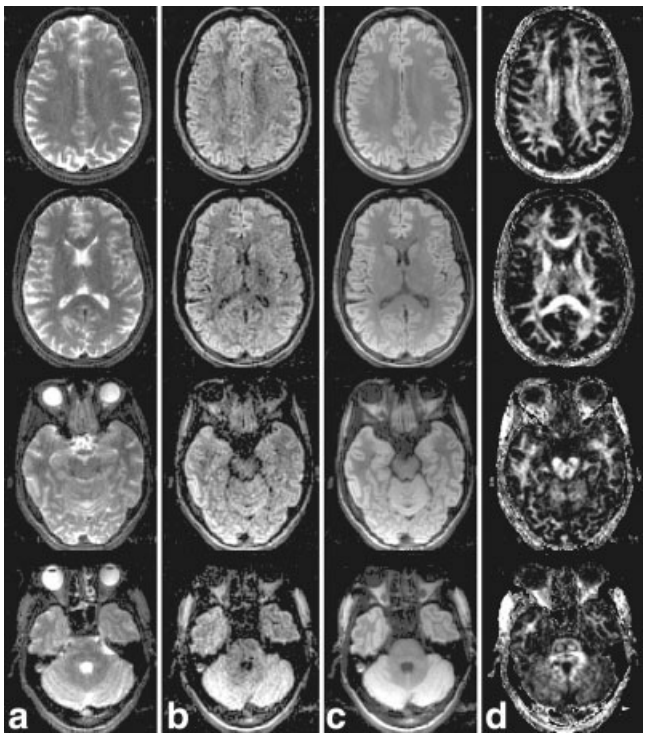

FIG. 5. **a:** Non-DW images, (**b**) DW images for a single diffusion direction $b(= 1000\,\mathrm{s\,mm^{-2}})$, (**c**) isotropically DW images, and (**d**) maps of the fractional anisotropy reconstructed from a four-segment DW MRI data set of the human brain with the proposed three-step method (four sections).

enhanced noise sensitivity of the ill-conditioned reconstruction problem for the undersampled segments affects the SNR of the final image. The least motion sensitivity and best SNR were obtained by adding another reconstruction by iterative linear inversion that exploits both the coil sensitivities from the first step and the motion-associated phase maps that may be extracted from the reconstructions of the second step. Because this third step uses the complementary *k*-space data from all segments, it is much better conditioned than the reconstructions from individual segments in the second step. The corresponding absence of any detectable noise amplification during the final reconstruction leads to a better SNR than obtainable by the two-step method.

In comparison with other reconstruction techniques for segmented motion-affected data sets, the main advantage of the proposed three-step method is the consideration of phase disturbances with high spatial frequencies. With respect to the work by Skare et al. (8), the approach further benefits from the high-quality coil sensitivities obtained by nonlinear inversion in the first step, the more flexible conjugate gradient-based version of the SENSE algorithm in the second step (see below), and the avoidance of any noise amplification in the third true reconstruction step.

The current implementation employed a Cartesian encoding scheme wherein each segment of both the non-DW and the DW acquisitions the center of *k*-space is fully sampled by eight or 16 lines. It should be noted, however, that the reference lines for the DW images are not necessarily required for the proposed three-step algorithm. Their use was originally motivated to allow for a fair comparison with the direct use of the nonlinear inversion technique, while later trials with reference lines and iterative SENSE-like reconstructions in the second and third step helped to improve the SNR. As far as non-DW images are concerned, the nonlinear inversion technique has already been demonstrated to be much less sensitive to a low number of central reference lines than conventional approaches (10).

In addition, also other specific aspects of the actual work such as the use of a full Fourier acquisition or even the choice of a Cartesian encoding scheme pose no general restrictions for the three-step method. Preliminary trials of both partial Fourier schemes and radial encoding schemes for the same segmented DW STEAM MRI sequence proved to be successful.

In order to be applicable, the proposed method has to meet only two experimental conditions: (i) the non-DW images must be reconstructable by nonlinear inversion, and (ii) each undersampled segment must contain enough data to allow for a reasonable reconstruction by parallel imaging, e.g., iterative SENSE. The first condition simply refers to the fact that the joint *k*-space of the non-DW images from all segments constitutes a fully sampled center. It is needed to properly estimate the coil sensitivities by regularized nonlinear inversion. The second condition requires the *k*-space lines in each segment of the DW images to be sampled in a sufficiently interleaved and dense manner to enable adequate reconstructions by parallel imaging. Apart from these requirements, however, the algorithm imposes no further constraints on the trajectory.

An interesting question arises for the dependence of the final image on the accuracy or noise of the estimated phase maps. For the experimental parameters chosen in this work, no difficulty was observed. In general, however, this may become a concern for very high reduction factors, that is, a large number of segments and a correspondingly ill-conditioned linear system. A possible solution may be to constrain the second reconstruction step by an even stronger regularization. Of note, the choice of regularization is not critical in the first and third step. Another possible source of reconstruction error may be due to alterations of the coil sensitivities that could occur due to severe macroscopic motions during the acquisition process. If this does not lead to a total corruption of the data set but emerges as a tractable problem, then a possible remedy may be obtained by using a regularized nonlinear inversion algorithm also in the second step. This would allow for a re-estimation of the coil sensitivities for each segment.

Finally, a most elegant algorithm to tackle the reconstruction problem in segmented DW MRI would be a regularized nonlinear inversion method that simultaneously treats coil sensitivities, motion-associated phase maps, and an object image as three independent unknowns. Such a method should achieve the same quality and robustness as the three-step algorithm proposed here but not suffer from the need to first reconstruct images from individual segments. Unfortunately, preliminary trials required a good initial guess for the phase maps, which so far renders the approach useless. Nevertheless, foreseeable

improvements of the algorithm are likely to alter the situation in future.

CONCLUSIONS

This work presents a new inverse reconstruction method for segmented multishot DW MRI that is based on the concepts of parallel imaging. Experimental applications deal with DW STEAM MRI of the human brain using three or four segments. The algorithm first determines separate coil sensitivity and motion-associated phase maps for each segment by taking advantage of the entire *k*-space data from multiple receiver coils. Subsequently, these maps are used to reconstruct object images without motion artifacts, again by parallel imaging based on the data from all segments. In contrast to existing approaches, the proposed method provides robust solutions without compromised SNR, even in cases where the phase variations are characterized by high spatial frequencies.

REFERENCES

1. Karaus A, Merboldt KD, Graessner J, Frahm J. Black-blood imaging of the human heart using rapid stimulated echo acquisition mode (STEAM) MRI. J Magn Reson Imaging 2007;26:1666–1671.
2. Miller KL, Pauly JM. Nonlinear phase correction of navigated diffusion imaging. Magn Reson Med 2003;50:343–353.
3. Liu C, Moseley ME, Bammer R. Simultaneous phase correction and SENSE reconstruction for navigated multi-shot DWI with non-Cartesian k-space sampling. Magn Reson Med 2005;54:1412–1422.
4. Atkinson D, Counsell S, Hajnal JV, Batchelor GP, Hill DLK, Larkman DJ. Nonlinear phase correction of navigated multi-coil diffusion images. Magn Reson Med 2006;56:1135–1139.
5. Pipe JG, Farthing VG, Forbes KP. Multishot diffusion-weighted FSE using PROPELLER MRI. Magn Reson Med 2002;47:42–52.
6. Liu C, Bammer R, Kim D, Moseley ME. Self-navigated interleaved spiral (SNAILS): application to high-resolution diffusion tensor imaging. Magn Reson Med 2004;52:1388–1396.
7. Nunes RG, Jezzard P, Behrens TEJ, Clare S. Self-navigated multishot echo-planar sequence for high-resolution diffusion-weighted imaging. Magn Reson Med 2005;53:1474–1478.
8. Skare S, Newbould RD, Clayton DB, Albers GW, Nagle S, Bammer R. Clinical multishot DW-EPI through parallel imaging with considerations of susceptibility, motion, and noise. Magn Reson Med 2007;57:881–890.
9. Ying L, Sheng J. Joint image reconstruction and sensitivity estimation in SENSE (JSENSE). Magn Reson Med 2007;57:1196–1202.
10. Uecker M, Hohage T, Block KT, Frahm J. Image reconstruction by regularized nonlinear inversion — application to autocalibrated parallel imaging. Magn Reson Med 2008;60:674–682.
11. Bakushinsky AB, Kokurin MY. Iterative methods for approximate solution of inverse problems. Dordrecht: Springer; 2004. p. 308.
12. Frahm J, Haase A, Matthaei D, Merboldt KD, Hänicke W. Rapid NMR imaging using stimulated echoes. J Magn Reson 1985;65:130–135.
13. Nolte UG, Finsterbusch J, Frahm J. Rapid isotropic diffusion mapping without susceptibility artifacts: whole brain studies using diffusion-weighted single-shot STEAM MR imaging. Magn Reson Med 2000;44:731–736.